AIAA-2002-3676

Laboratory Model 50kW Hall Thruster

David H. Manzella
University of Toledo
Toledo, Ohio 43606

Robert S. Jankovsky
NASA Glenn Research Center
Cleveland, Ohio 44135

Richard R. Hofer
QSS Group, Inc.
Cleveland, Ohio 44135

38th AIAA Joint Propulsion Conference
7-10 July 2002
Indianapolis, Indiana

Laboratory Model 50 kW Hall Thruster

David Manzella
The University of Toledo
Toledo, OH 43606

Robert Jankovsky
NASA Glenn Research Center
Cleveland, OH 44135

Richard Hofer
QSS Group, Inc.
Cleveland, OH 44135

A 0.46 meter diameter Hall thruster was fabricated and performance tested at powers up to 72 kilowatts. Thrusts up to 2.9 Newtons were measured. Discharge specific impulses ranged from 1750 to 3250 seconds with discharge efficiencies between 46 and 65%. Overall specific impulses ranged from 1550 to 3050 seconds with overall efficiencies between 40 and 57%. Performance data indicated significant fraction of multiple-charged ions during operation at elevated power levels. Cathode mass flow rate was shown to be a significant parameter with regard to thruster efficiency.

Introduction

High power electric propulsion systems have been shown to enable a number of missions including missions to Mars and Earth orbital solar electric power generation for terrestrial use.[1,2] These types of missions require moderate transfer times and sizable thrust levels resulting in an optimized propulsion system specific impulse from 2000-3000 seconds based on the available on-board power. Hall thruster technology offers a favorable combination of performance, reliability, and lifetime for such applications based on the characteristics of state-of-the-art systems. As a result, the NASA Space Solar Power Concept and Technology Maturation Program initiated preliminary strategic technology research and development into high power Hall thruster technology to enable space solar power systems and other high power spacecraft.

High power Hall thruster technology for primary propulsion applications was initially investigated in the former Soviet Union and later Russia for interplanetary missions.[3,4] Efforts conducted at the FAKEL Design Bureau in Kaliningrad, Russia culminated in the SPT-290. This thruster utilized a 290 mm outer diameter ceramic channel to ultimately produce as much as 1.1 Newtons of thrust at 25 kilowatts of input power using xenon as the propellant. Efforts at the Central Scientific Institute for Machine Building (TsNIIMASH) in Korolev, Russia resulted in the demonstration of a 100 kilowatt two-stage anode layer thruster demonstrating a specific impulse of 8000 seconds with a discharge efficiency of 80% using bismuth as the propellant. Later a xenon fueled anode layer thruster was tested at power levels up to 25 kilowatts demonstrating performance similar to the SPT-290 at that power level.[5] More recently an SPT-type thruster designated the T-220, which was developed in the United States under contract to NASA Glenn Research Center by TRW in cooperation with Space Power Incorporated (who has since become a part of Pratt & Whitney's Space Propulsion and Chemical Systems Division), was tested.[6] This thruster which has a 220 mm outer diameter ceramic channel was originally designed to produce 0.5 Newtons of thrust at 10 kW but has been modified to produce in excess of 1 Newton of thrust at elevated power levels.[7]

Development of a Hall thruster capable of operating at 2000-3000 seconds at power levels of 50 kilowatts and above requires a thruster design which preserves the physical processes required for efficient ionization and acceleration of the propellant. Important characteristics for preservation of these processes include: discharge current density, discharge chamber geometry, and magnetic field distribution.[8] This paper describes the development of a Hall thruster designed to operate at 50 kilowatts. Test results including the effect of discharge voltage, anode mass flow rate and cathode mass flow rate on thruster performance are included.

Apparatus

A photograph of the NASA-457M 50-kilowatt laboratory Hall thruster is shown in Figure 1. The thruster, which has a 457 mm outer diameter ceramic discharge chamber, injects xenon propellant into the rear of the channel through a series of holes located

along the inner and outer walls of the annular metallic anode located at the rear of the channel. The cathode, which has been previously described,[9] was located on the thruster centerline.

A magnetic field is established across the exit plane of the discharge chamber through the use of two concentric electromagnets. Each electromagnet can be independently powered. The electromagnets along with magnetic poles and screens form the magnetic circuit. The design of the magnetic circuit was optimized through the use of a commercial three-dimensional magneto-static computer code, Magnet 6 by Infolytica. The field line topography employed in the NASA 457M is qualitatively similar to the plasma lens design of the NASA 173M.[10] Following fabrication of the thruster the results from the magnetic model were compared with magnetic intensities measured with a 3-axis Gauss meter. The measured and calculated radial and axial components of the magnetic field are shown in Figure 2. The channel depth normalized the axial distance and both the radial and axial magnetic field components were normalized by the maximum values respectively. The inner radial magnetic field strength was slightly higher than calculated which also affected the centerline radial field strength. This difference was attributed to uncertainty in the properties of the material used in this part of the magnetic circuit.

The thruster was tested in a cryogenically pumped cylindrical vacuum chamber measuring 5 meters in diameter by 20 meters in length. This facility, which has been described in detail previously,[10] was modified for this test. A cylindrical test port measuring 2 meters in diameter by 2.5 meters in length was mounted along the major axis of the tank with a 2-meter isolation valve between the test port and the main volume of the tank. A photograph of the test facility is shown in Figure 3. The effective pumping speed of the test facility in this configuration was 700,000 liters per second. This was determined based on the xenon mass flow rate and the tank pressure measured behind the thruster. As a result, the highest background pressure was $2x10^{-5}$ Torr at a xenon flow rate of just over 1 standard liter per minute (SLPM). This pressure is still below the maximum recommended value for performance testing of $5x10^{-5}$ Torr.[11] A laboratory xenon feed system, required auxiliary power supplies, and a data acquisition system were located adjacent to the test port on an elevated deck platform that was also modified for these tests. The discharge power supply was a remotely located three phase commercially available unit with a rated output of 100 Amperes and 2000 Volts. An output filter consisting of a 21mF capacitor located between the anode and cathode was used. The thrust produced by the NASA-457M was measured using an inverted pendulum design thrust stand fabricated specifically for these tests. The thrust stand was designed based on a thrust stand used in previous evaluations of Hall effect thrusters.[12,13] Conceptually the thrust balance was identical to the previous design except for modifications necessary to accommodate the increased mass and currents. The thrust stand can be seen beneath the thruster in the photograph in Figure 4. Due to the large thermal mass of the NASA-457M thruster no attempts were made to establish complete thermal equilibrium prior to measuring performance data. The thruster was typically operated for approximately an hour to allow not only the thruster discharge chamber to warm up, but to also allow the thrust stand to equilibrate with the operating thruster. Following this warm up period performance data was taken. Thrust stand calibrations, conducted by applying a series of one hundred gram weights, were conducted before and after each series of test data.

Results and Discussion

The NASA-457M was tested over a range of input powers from 9 to 72 kilowatts by varying the anode mass flow rate from 15 to 93 mg/s and the discharge voltage from 300 to 650 Volts. All these data are presented in an appendix at the end of this paper. Over this range of operating conditions thruster operation was stable. Thrust is plotted as a function of discharge power for five different discharge voltages in Figure 5. For each voltage the maximum current corresponded to approximately 110 Amperes. This maximum resulted from the maximum current capacity of the discharge power supply. As can be seen from the figure, thrust varied linearly with discharge power for a given discharge voltage. At 650 Volts a thrust of 2.9 Newtons was measured at 111 Amperes. There was no evidence of thermal limitations at this power level although it was noted that the anode was glowing upon shutdown. While this has been observed with other thrusters operating at nominal operating conditions at shutdown, this was not observed at powers up to 50 kW with the NASA-457M. Operation at voltages above 650 Volts was investigated but was not adequately characterized due to voltage isolation problems within the thruster. Modification of the isolation scheme is currently underway which should allow for operation up to at 1000 Volts for future testing.

The reduction in thrust with increasing voltage at a given power level was accompanied by a corresponding increase in specific impulse. This is shown in Figure 6 where specific impulse is plotted versus discharge power. Discharge specific impulse

ranged from approximately 1750 seconds to 3250 seconds. The overall thruster specific impulse including the cathode mass flow rate and magnet power ranged from 1550 seconds to 3050 seconds. While overall specific impulse and efficiency are reported, it should be noted that no attempts were made to optimize the laboratory model cathode or magnetic circuit for efficient operation. The discharge specific impulse at a given voltage compares favorably with other state-of-the-art thrusters. For example at 300 Volts an SPT-100 has a discharge specific impulse of 1750 seconds[14] and the comparably sized high voltage SPT-1 thruster provided between 2250 and 2500 seconds at 500 Volts.[15] The functional dependence of specific impulse with discharge voltage was considered in more detail by Hofer where experimental data were compared with various predicted values.[16] These predictions suggest as discharge power increased above 20 kilowatts or the discharge current increased above 30 Amperes that the effect of multiple-charged ions becomes significant.

The variation of discharge current versus anode mass flow rate is shown in Figure 7. The dependence is linear for anode mass flow rates below approximately 70 mg/s. Above this mass flow rate the discharge current increased more rapidly with increasing anode mass flow rate. This increase in current at high anode mass flow rate was the result of either an increase in the electron or ion current contribution to the discharge current. The corresponding specific impulse and higher density within the channel suggest that this effect is due to additional ion current from multiple-charged ions.

The effect of multiple charged ions on specific impulse was previously considered when Hofer predicted 100 Amperes at 88.8 mg/s and 500 Volts with a 2768 second specific impulse for a multiple-charged plasma. For a singly charged plasma 100 Amperes at 101 mg/s and 500 Volts with a 2622 second specific impulse was predicted. The measured anode mass flow rate at 500 Volts and 100 Amperes was 86.4 mg/s at just less than 2750 seconds, which agrees favorably with the multiple-charged prediction. This prediction and other predicted values of specific impulse are shown in Figure 8 versus discharge voltage for an anode mass flow rate of 86.4 mg/s. Experimental data are also included.

During the course of this investigation the effect of cathode flow rate on thruster performance was also considered. Previously the sensitivity of cathode mass flow rate on thruster operation was considered in detail for a 4.5 kW Hall thruster.[17] As was pointed out in this prior investigation, the coupling of the plasma produced in the hollow cathode with the plasma produced in the Hall thruster discharge channel is not fully understood and is more complicated than running a hollow cathode with a simple external anode due to the presence of magnetic fields. Figure 9 shows the cathode-to-ground voltage as a function of discharge current for three different cathode flow rates. As can be seen from the figure, for each cathode flow rate the cathode-to-ground voltage varied linearly with discharge current with the voltage becoming more negative with increasing current.

For comparison purposes, this cathode was tested independent of the Hall thruster with an external anode at a mass flow rate of 2 mg/s.[9] For currents between 50 and 100 Amperes the coupling voltage was between -10 and -13 volts. This suggests that the additional voltage required to couple the plasma from the cathode to the plasma from the Hall thruster was associated with electron transport across the applied magnetic field. As such, this additional voltage represents a thruster loss mechanism since a larger portion of the voltage applied between the cathode and anode is needed for cathode coupling leaving a smaller portion of the total applied voltage for ion acceleration.

The effect of large cathode-to-ground coupling voltages on thruster discharge efficiency is shown in Figure 10. These data show that the smaller the cathode-to-ground voltage the higher the discharge efficiency (and overall efficiency as can be seen in the data tables). This substantiates the conclusion that large cathode-to-ground voltages were indicative of an energy loss mechanism associated with poor cathode coupling. The data also indicate a peak discharge efficiency of near 65% at around 500 Volts. The efficiency decreases with increasing voltage above this value. This is consistent with past investigations into high voltage Hall thruster operation.[15,18]

Conclusions

A 0.46 m outer diameter Hall thruster was fabricated and performance tested at powers up to 72 kilowatts. These tests demonstrated the efficacy of scaling Hall thrusters to high power suitable for a range of future missions. Thrusts up to nearly 3 Newtons were measured. Discharge specific impulses ranged from 1750 to 3250 seconds with discharge efficiencies between 46 and 65%. Overall specific impulses ranged from 1550 to 3050 seconds with overall efficiencies between 40 and 57%.

Performance data suggested a significant fraction of multiple-charged ions during operation at elevated

power levels. This conclusion was supported by previous performance predictions by Hofer and the functional dependence of discharge current with anode mass flow rate.

An investigation into the effect of cathode flow rate on thruster operation was conducted. Cathode mass flow rate was shown to be a significant parameter with regard to thruster efficiency. It was also demonstrated that the coupling voltage between the cathode and thruster anode was significantly different than that measured with the cathode operating to a planar external anode.

References

1. Gefert, L., Hack, K., and Kerslake, T., "Options for the Human Exploration of mars Using Solar Electric Propulsion," 1999.
2. Oleson, S., "Advanced Propulsion for Space Solar Power Satellites," AIAA-99-2872, June 1999.
3. Loeb, H. and Popov, G., "Advanced Interplanetary Mission of the XXI Century Using Electric Propulsion," IEPC-95-04, Sept. 1995.
4. Garkusha, V., et. al., "Electric Propulsion Activity in TsNIIMASH," IEPC-95-09, Sept. 1995.
5. Jacobson, D. and Jankovsky, R., "Performance Evaluation of a 50 kW Hall Thruster," AIAA-99-0457, January 1999.
6. Jankovsky, R., McLean, C., and McVey, J., "Preliminary Evaluation of a 10kW Hall Thruster," AIAA-99-0456, January 1999.
7. Britt, N., "Electric Propulsion Activities in US Industry," AIAA-2002-3559, July 2002.
8. Arkhipov, B., et. Al., "Development and Investigation of Characteristics of Increased Power SPT Models," IEPC-93-222, Sept. 1993.
9. Carpenter, C. and Patterson, M., "High-Current Hollow cathode Development," IEPC-01-274, October 2001.
10. Hofer, R. R., Peterson, P. Y., Gallimore, A. D., "A High Specific Impulse Two-Stage Hall Thruster with Plasma Lens Focusing," IEPC-01-036, 27th International Electric Propulsion Conference, Pasadena, CA, Oct 14-19, 2001.
10. Grisnik, S., and Parkes, J., "A Large High Vacuum, High Pumping Speed Space Simulation Chamber for Electric Propulsion," IEPC-93-151, Sept. 1993.
11. Randolph, T. et.al., "Facility Effects on Stationary Plasma Thruster Testing," IEPC-93-93, Sept. 1993.
12. Sankovic, J.M., Haag, T.W., and Manzella, D.H., "Operating Characteristics of the Russian D-55 Thruster with Anode Layer," AIAA-94-3011, June 1994.
13. Sankovic, J.M., Haag, T.W., and Manzella, D.H., "Performance Evaluation of a 4.5 kW SPT Thruster, " IEPC-95-30, Sept. 1995.
14. Kim, V. et al, "Development and Characterization of Small SPT," AIAA-98-3335, July 1998.
15. Manzella, D., Jacobson, D., and Jankovsky, R., "High Voltage SPT Performance," AIAA-2001-3774, July 2001.
16. Hofer, R. and Jankovsky, R., "A Hall Thruster Performance Model Incorporating the effects of a Multiply-Charged Plasma," AIAA-2001-3322, July 2001.
17. Tilley, D., de Grys, K., and Myers, R., "Hall Thruster – Cathode Coupling," AIAA-99-2865, June 1999.
18. Jacobson, D., Jankovsky, R., and Manzella, D., "High Voltage TAL Performance," AIAA-2001-3777.

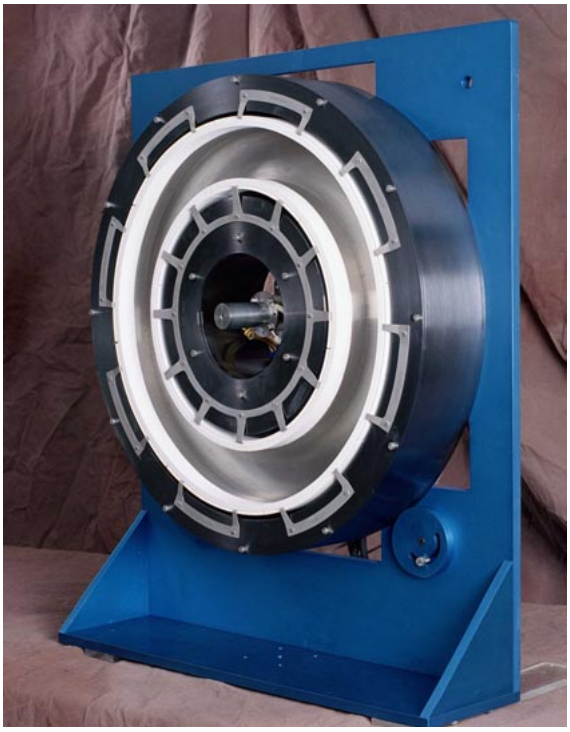

Figure 1: Photograph of the NASA-457M high power Hall thruster

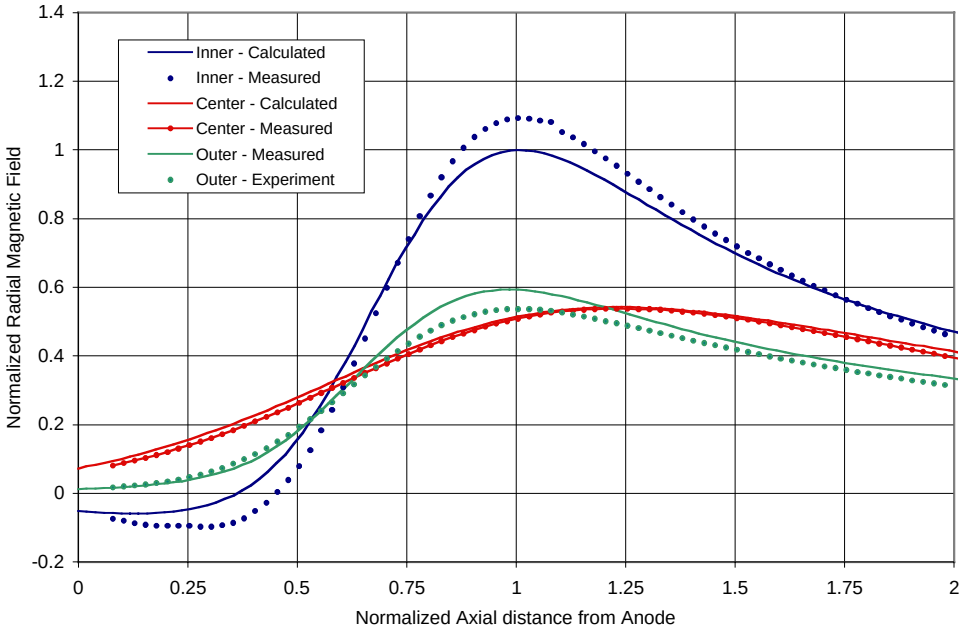

Figure 2a: Measured and predicted radial magnetic field strength

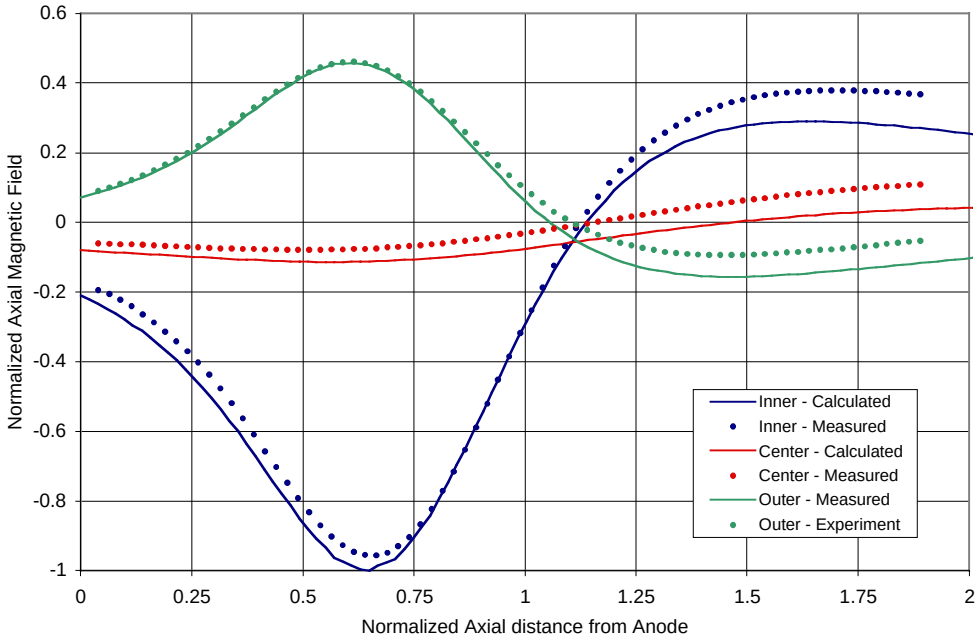

Figure 2b: Measured and predicted axial magnetic field strength

Figure3: Photograph test facility showing new test port

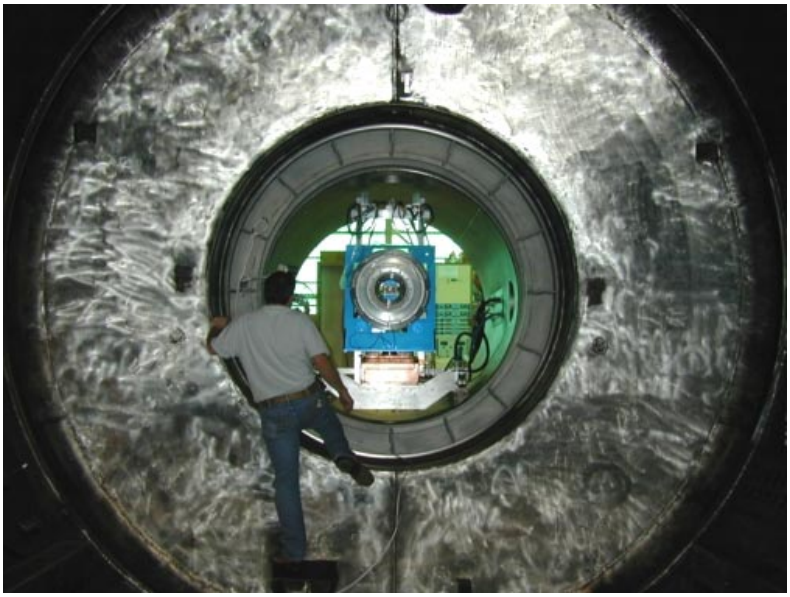

Figure 4: Photograph of thruster mounted on thrust stand in test port

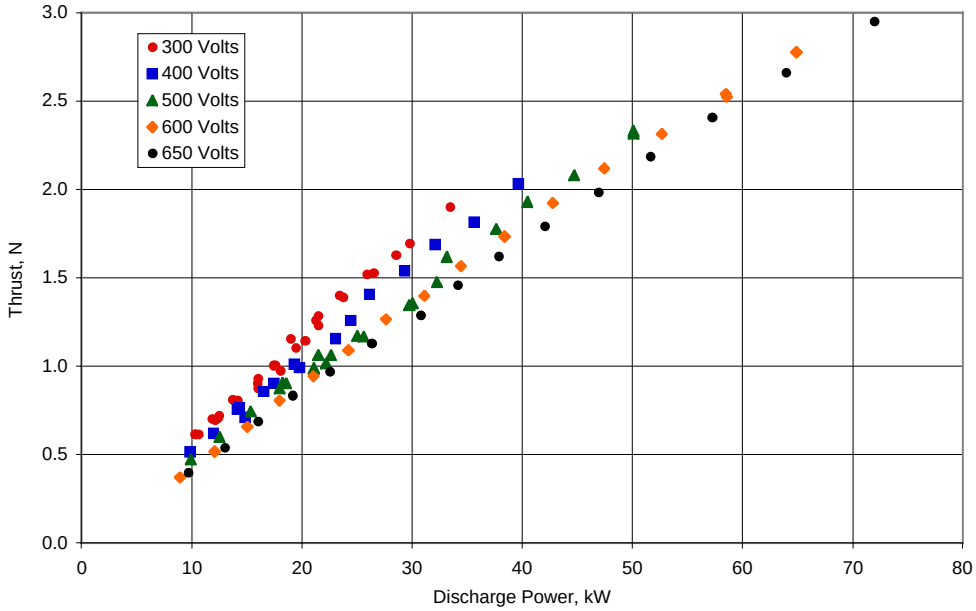

Figure 5: Thrust versus discharge power for various discharge voltages

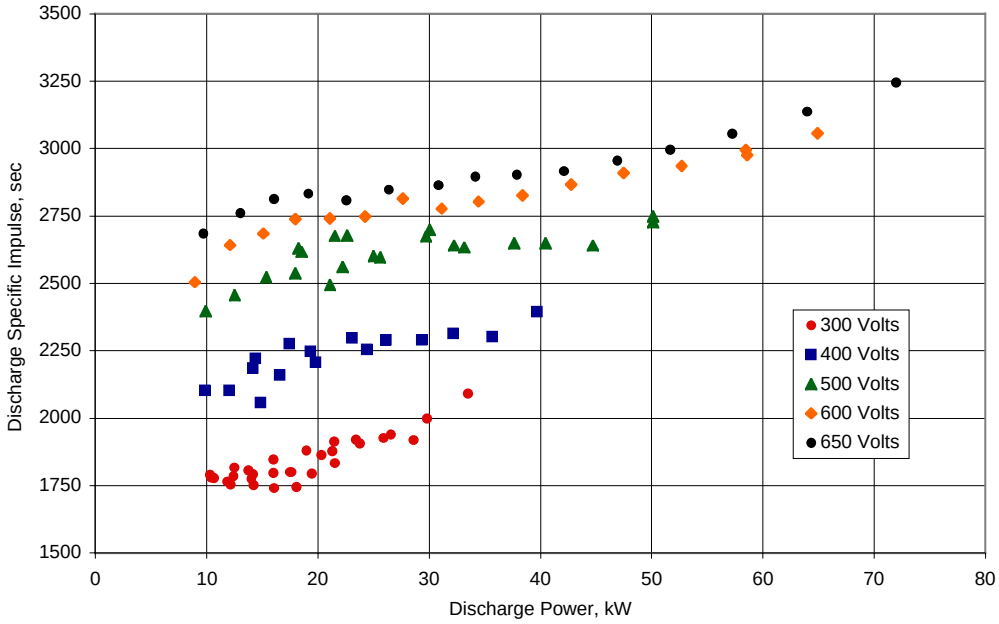

Figure 6: Discharge specific impulse versus discharge power for various discharge voltages

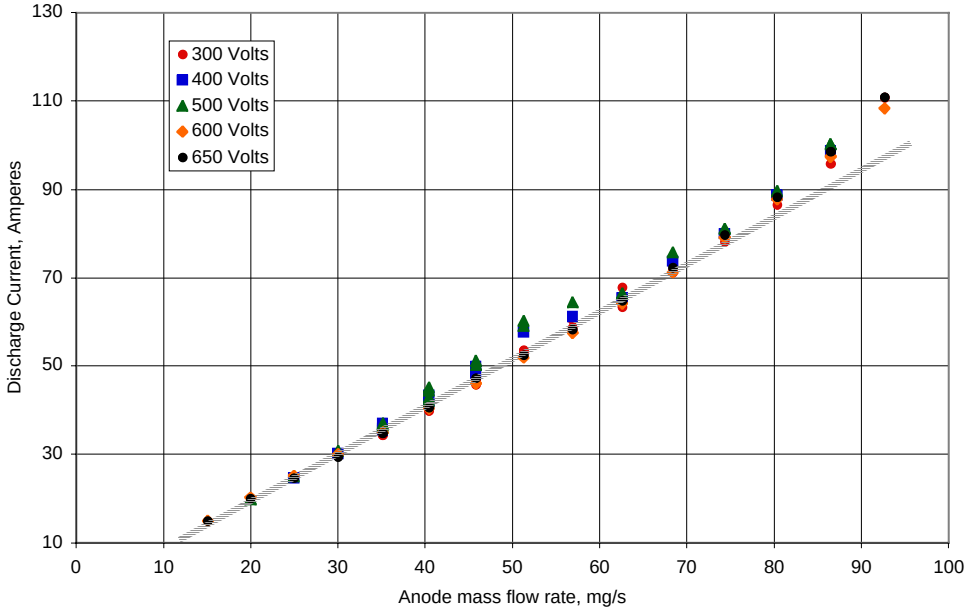

Figure 7: Discharge current versus anode mass flow rate for various discharge voltages

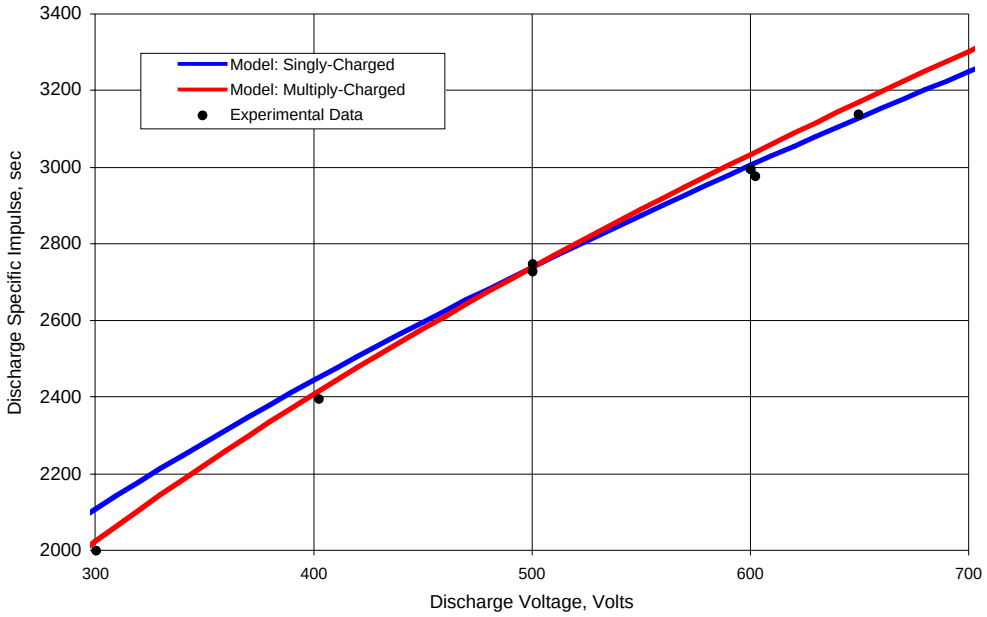

Figure 8: Predicted and measured specific impulse versus discharge voltage for an anode mass flow rate of 86.4 mg/s

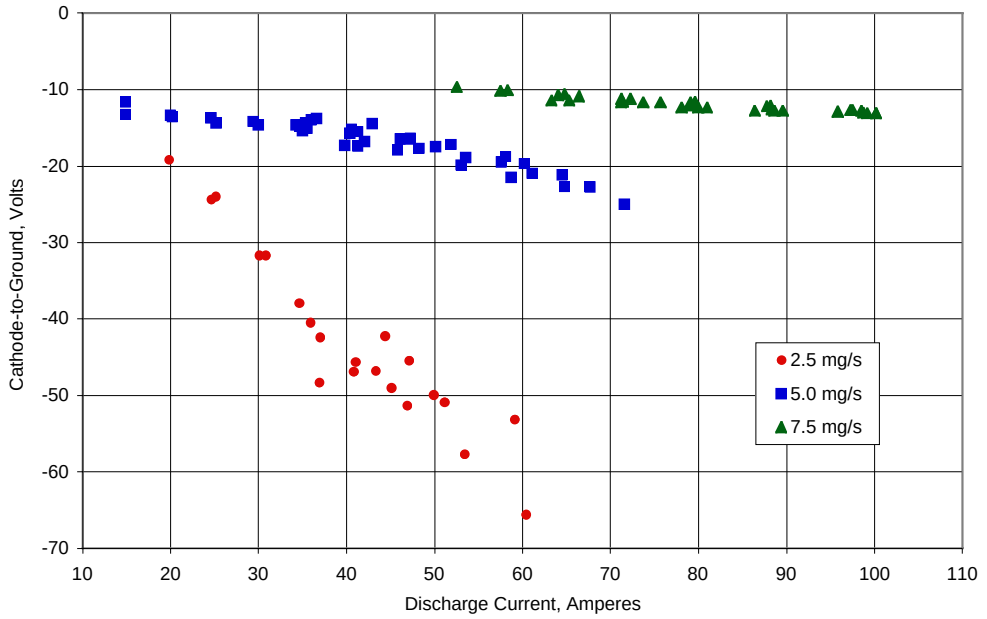

Figure 9: Cathode-to-ground voltage versus discharge current for various cathode flow rates.

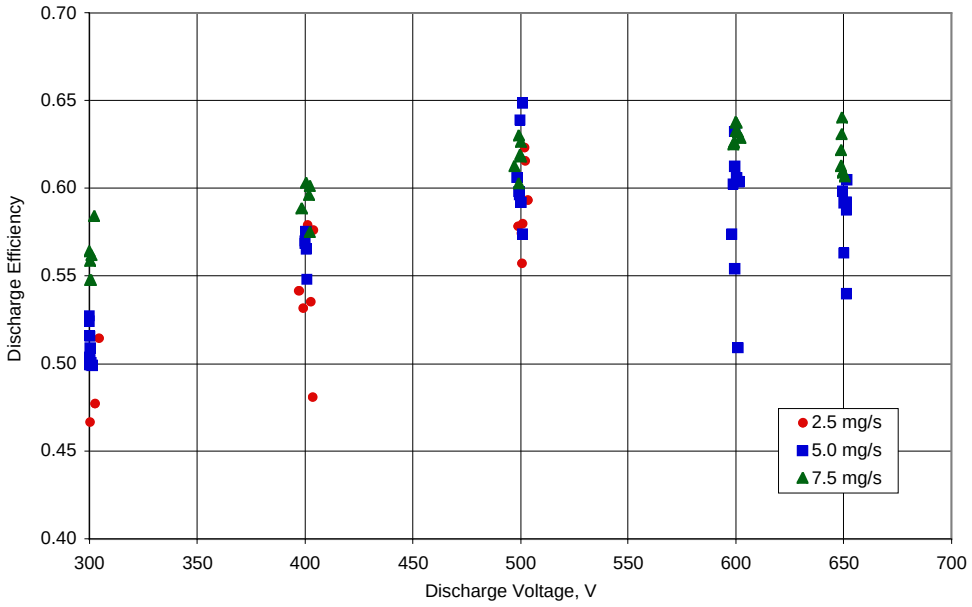

Figure10: Discharge efficiency versus discharge current for various cathode flow rates.

Appendix: Data Table

Discharge voltage Volts	Discharge current Amperes	Discharge power Watts	Anode mass flow mg/s	Cathode mass flow mg/s	Total power Watts	Thrust mN	Total specific impulse seconds	Discharge specific impulse seconds	Total efficiency	Discharge efficiency	Cathode-to-ground voltage Volts
300	34	10287	35.2	5.0	11348	617	1567	1790	0.42	0.53	-14.6
300	35	10383	35.2	2.5	11483	614	1662	1781	0.44	0.52	-37.9
300	36	10661	35.2	5.0	11606	613	1557	1778	0.40	0.50	-15.1
299	40	11880	40.4	5.0	12961	701	1572	1766	0.42	0.51	-17.3
298	41	12150	40.4	2.5	13052	696	1653	1755	0.43	0.49	-46.9
304	41	12480	40.4	2.5	13735	721	1711	1817	0.44	0.51	-45.6
301	41	12411	40.4	5.0	13385	709	1590	1786	0.41	0.50	-15.5
300	46	13740	45.8	5.0	15010	812	1629	1807	0.43	0.52	-17.9
302	47	14183	45.8	2.5	15116	787	1661	1752	0.42	0.48	-51.3
298	47	14012	45.8	2.5	15015	798	1684	1776	0.44	0.50	-45.4
301	47	14168	45.8	5.0	15164	806	1617	1793	0.42	0.50	-16.5
301	53	15974	51.3	5.0	16999	904	1637	1796	0.43	0.50	-19.9
300	53	16031	51.3	2.5	16985	876	1660	1741	0.42	0.47	-57.7
299	54	16010	51.3	5.0	17358	930	1683	1847	0.44	0.53	-18.9
300	58	17453	56.9	5.0	18772	1005	1655	1801	0.43	0.51	-18.8
300	59	17622	56.9	5.0	18675	1005	1655	1801	0.44	0.50	-21.5
299	60	18078	56.9	2.5	19071	974	1671	1745	0.42	0.46	-65.6
300	63	18971	62.6	7.5	19643	1155	1679	1881	0.48	0.56	-11.4
300	65	19459	62.6	5.0	20542	1103	1663	1796	0.44	0.50	-22.7
300	68	20290	62.6	5.0	21664	1145	1726	1864	0.45	0.52	-22.8
299	71	21275	68.4	7.5	22400	1261	1694	1879	0.47	0.55	-11.7
301	71	21481	68.4	7.5	22829	1285	1726	1915	0.48	0.56	-11.6
300	72	21494	68.4	5.0	22596	1231	1710	1835	0.46	0.52	-25
300	78	23422	74.3	7.5	24701	1401	1746	1922	0.49	0.56	-12.4
300	79	23754	74.3	7.5	24901	1390	1732	1907	0.47	0.55	-12.1
300	86	25894	80.3	7.5	27194	1519	1763	1928	0.48	0.55	-12.8
301	88	26543	80.3	7.5	27707	1528	1774	1939	0.48	0.55	-12.6
298	96	28587	86.4	7.5	29923	1629	1767	1921	0.47	0.54	-12.9
300	99	29780	86.4	7.5	30970	1696	1840	2000	0.49	0.56	-13.1
302	111	33454	92.7	7.5	34663	1903	1937	2093	0.52	0.58	-13.7

Discharge voltage Volts	Discharge current Amperes	Discharge power Watts	Anode mass flow mg/s	Cathode mass flow mg/s	Total power Watts	Thrust mN	Total specific impulse seconds	Discharge specific impulse seconds	Total efficiency	Discharge efficiency	Cathode-to-ground voltage Volts
403	25	9904	24.9	2.5	10800	514	1911	2103	0.45	0.54	-24.4
399	30	12016	30.0	2.5	13084	619	1942	2104	0.45	0.53	-31.7
400	35	14164	35.2	5.0	15255	753	1912	2184	0.46	0.57	-14.4
401	36	14399	35.2	2.5	15556	766	2072	2220	0.50	0.58	-40.5
403	37	14885	35.2	2.5	16286	710	1921	2057	0.41	0.48	-48.3
401	41	16561	40.4	5.0	17747	857	1922	2160	0.46	0.55	-17.4
404	43	17485	40.4	2.5	18762	903	2143	2276	0.51	0.58	-46.8
401	48	19349	45.8	5.0	20643	1010	2025	2247	0.49	0.58	-17.7
397	50	19815	45.8	2.5	21055	992	2093	2207	0.48	0.54	-49.9
401	58	23080	51.3	5.0	24442	1157	2095	2299	0.49	0.57	-19.5
400	61	24446	56.9	5.0	25784	1258	2071	2253	0.50	0.57	-21
401	65	26159	62.6	7.5	26867	1405	2044	2289	0.52	0.60	-11.4
399	74	29377	68.4	7.5	30743	1538	2065	2292	0.51	0.59	-11.7
402	80	32144	74.3	7.5	33446	1688	2103	2315	0.52	0.60	-12.4
402	89	35653	80.3	7.5	36971	1815	2106	2303	0.51	0.57	-12.8
402	99	39697	86.4	7.5	41050	2031	2204	2395	0.53	0.60	-13
501	20	9912	20.0	2.5	10641	470	2131	2398	0.46	0.56	-19.2
499	25	12517	24.9	2.5	13462	601	2233	2457	0.49	0.58	-24
499	31	15382	30.0	2.5	16476	743	2330	2524	0.51	0.60	-31.7
499	36	17950	35.2	5.0	19078	875	2220	2536	0.50	0.61	-14
500	37	18293	35.2	5.0	19483	907	2301	2628	0.53	0.64	-13.8
502	37	18570	35.2	2.5	19765	902	2442	2615	0.55	0.62	-42.4
501	42	21092	40.4	5.0	22304	989	2220	2494	0.48	0.57	-16.8
501	43	21497	40.4	5.0	22709	1062	2382	2676	0.55	0.65	-14.5
500	44	22218	40.4	2.5	23323	1016	2412	2561	0.52	0.57	-42.2
502	45	22649	40.4	2.5	23942	1062	2521	2677	0.55	0.62	-49
500	50	25030	45.8	5.0	26341	1170	2346	2602	0.51	0.60	-17.5
501	51	25601	45.8	2.5	26742	1166	2460	2595	0.53	0.58	-50.9
504	59	29757	51.3	2.5	30932	1346	2550	2674	0.54	0.59	-53.1
499	60	30064	51.3	5.0	31435	1358	2459	2698	0.52	0.60	-19.7
500	65	32269	56.9	5.0	33631	1474	2428	2641	0.52	0.59	-21.2
499	66	33154	62.6	7.5	33898	1617	2352	2633	0.55	0.63	-10.9
497	76	37646	68.4	7.5	39028	1776	2385	2647	0.53	0.61	-11.7
500	81	40484	74.3	7.5	41806	1930	2405	2648	0.54	0.62	-12.4
499	90	44737	80.3	7.5	46074	2081	2415	2641	0.54	0.60	-12.8
500	100	50120	86.4	7.5	51483	2330	2528	2747	0.56	0.63	-13.1
500	100	50120	86.4	7.5	51483	2314	2511	2728	0.55	0.62	-13.1
601	15	8956	15.1	5.0	10022	371	1881	2504	0.34	0.51	-11.6
599	20	12108	20.0	5.0	13190	518	2113	2642	0.41	0.55	-13.6
598	25	15075	24.9	5.0	16174	657	2237	2686	0.45	0.57	-14.4
599	30	17964	30.0	5.0	19080	806	2347	2738	0.49	0.60	-14.6
602	35	21056	35.2	5.0	22191	945	2400	2741	0.50	0.60	-15.4
600	40	24256	40.4	5.0	25408	1090	2446	2748	0.51	0.61	-15.7
600	46	27637	45.8	5.0	28801	1265	2538	2815	0.55	0.63	-16.5
600	52	31119	51.3	5.0	32295	1398	2532	2778	0.54	0.61	-17.2
599	58	34431	56.9	7.5	35626	1565	2477	2804	0.53	0.62	-10.2
599	64	38415	62.6	7.5	39625	1735	2523	2826	0.54	0.63	-10.7
601	71	42777	68.4	7.5	43996	1923	2583	2866	0.55	0.63	-11.2
600	79	47468	74.3	7.5	48699	2121	2642	2909	0.56	0.64	-11.7
600	88	52680	80.3	7.5	53923	2314	2685	2936	0.57	0.63	-12.2
602	97	58594	86.4	7.5	59792	2524	2738	2976	0.57	0.63	-12.7
600	98	58500	86.4	7.5	59755	2540	2756	2995	0.57	0.64	-12.7
599	108	64915	92.7	10.0	66127	2778	2758	3055	0.57	0.64	-13.6
651	15	9706	15.1	5.0	10599	398	2017	2684	0.37	0.54	-13.3
650	20	13006	20.0	5.0	13920	541	2208	2761	0.42	0.56	-13.4
651	25	16022	24.9	5.0	16953	688	2343	2813	0.47	0.59	-13.7
652	29	19157	30.0	5.0	20115	834	2429	2834	0.49	0.60	-14.2
650	35	22562	35.2	5.0	23541	969	2459	2809	0.50	0.59	-14.8
650	41	26370	40.4	5.0	27368	1129	2534	2847	0.51	0.60	-15.2
651	47	30811	45.8	5.0	31826	1288	2584	2866	0.51	0.59	-16.4
651	53	34151	51.3	7.5	35231	1458	2527	2897	0.51	0.61	-9.7
650	58	37878	56.9	7.5	38982	1621	2565	2904	0.52	0.61	-10.1
650	65	42088	62.6	7.5	43213	1791	2605	2917	0.53	0.61	-10.6
649	72	46915	68.4	7.5	48058	1983	2664	2956	0.54	0.61	-11.2
649	80	51644	74.3	7.5	52840	2184	2722	2996	0.55	0.62	-11.6
649	88	57242	80.3	7.5	58454	2409	2796	3057	0.57	0.63	-12.1
649	99	63956	86.4	7.5	65182	2661	2888	3138	0.58	0.64	-12.8
649	111	71963	92.7	10.0	73201	2950	2929	3245	0.58	0.65	-13.9